Fluid Dynamics & Materials Processing
DOI:10.32604/fdmp.2020.010951
Article

Tech Science Press

Heat Transfer Enhancement Using R1234yf Refrigerants in Micro-Ribbed Tubes in a Two-Phase Flow Regime

Daoming Shen[1,*], Xia Zhang[1], Wei He[1], Jinhong Xia[1] and Songtao Xue[2]

[1]School of Civil Engineering & Architecture, Xinxiang University, Xinxiang, China
[2]Department of Architecture, Tohoku Institute of Technology, Sendai, 982-8577, Japan
*Corresponding Author: Daoming Shen. Email: shen2019@xxu.edu.cn
Received: 09 April 2020; Accepted: 24 October 2020

Abstract: Experiments about heat transfer in the presence of a two-phase flow due to the condensation of a R1234yf refrigerant have been performed considering a smooth tube and two micro-fin tubes. The following experimental conditions have been considered: Condensation temperatures of 40°C, 43°C and 45°C, mass fluxes of 500–900 kg/(m^2·s), vapor qualities at the inlet and outlet of the heat transfer tube in the ranges 0.8–0.9 and 0.2–0.3, respectively. These tests have shown that: (1) The heat transfer coefficient increases with decreasing the condensation temperature and on increasing the mass flux; (2) The heat transfer coefficient inside the micro-fin tube is larger than that for the smooth tube; (3) The heat transfer enhancement factors for the micro-fin tube with a fin helical angle of 8° and 15° are 2.51–2.89 and 3.11–3.57, respectively; both are higher than the area increase ratio. These experimental results have been compared with correlations available in the literature: the Cavallini et al. correlation has the highest accuracy in predicting the heat transfer coefficient inside the smooth tube, the related percentage error and the average prediction error are ±8% and 0.56%, respectively; for the micro-fin tube these become ±25% and 6%, respectively.

Keywords: R1234yf; micro-ribbed tube; heat transfer coefficient; heat transfer enhancement factor

1 Introduction

With the deepening of energy crisis and deterioration of the environmental pollution, energy-saving, efficient and miniaturized internal threaded tubes are widely applied in diverse industrial heat exchangers, including evaporators and condensers in refrigeration systems [1,2]. Studies show that synthetic refrigerants have caused serious environmental problems correlated to global warming and ozone-depleting effects. These problems are especially more pronounced over the past few decades. Therefore, in order to prevent further environmental damage, applying natural and eco-friendly substances in the refrigeration is highly demanded. The inner fin of the micro-finned tube enlarges the heat transfer surface area of the tube so that it enhances the turbulence of the fluid in the tube, thereby improving the heat transfer efficiency [3,4]. Wu et al. [5] found that the heat transfer coefficient in the micro-finned tube is about 90% higher than that in the smooth tube. They showed that the improvement in the heat transfer coefficient is much higher than that of the area ratio (40%).

Moreover, Zheng et al. [6] studied the effects of structural parameters such as the helical angle of fins, number of fins and the top angle of teeth on the heat transfer characteristics in tubes. Tang et al. [7] made a comparative analysis of the heat transfer coefficients of the smooth tube and micro-ribbed tube.

Krishnan et al. [8] investigated the combined effect of the convective heat transfer and analyzed the entropy generation in the solution of magnesia nanoparticles derived from the combustion synthesis dispersed in ethylene glycol-water flowing through a micro-fin tube heat exchanger. Kedzierski et al. [9] studied the local convective boiling heat transfer and fanning friction factor measurements in a micro-fin tube for refrigerant R134a. Moreover, they proposed two possible low global warming potential (GWP) refrigerant replacements for R134a, namely R1234yf and R450A.

It is worth noting many theoretical investigations have been conducted so far on the flow and condensation heat transfer characteristics in smooth and Micro-finned tubes. For example, Thome et al. [10] categorized heat transfer zones into dry and wet zones based on experiments of the flow condensation heat transfer in smooth tubes. They applied different refrigerants, including R11, R12, R22, R32 and R113 in the experiments. Then, they compared the calculation models of heat transfer coefficients in different zones. Jung et al. [11] established a correlation between two-phase and single-phase heat transfer coefficients based on the condensation heat transfer coefficients of refrigerants R12, R22, R32, R123, R125 and R134a. Cavallini et al. [12] and Oliver et al. [13] used dimensionless Rx to characterize the effect of fins on the flow pattern in tubes. Then, based on the condensation experimental data of R22 and R410A, they established a correlation between the heat transfer coefficient and dimensionless parameters. Miyara et al. [14] and Kim et al. [15] demonstrated that fins mainly enhance the forced convection heat transfer of the fluid in tubes. They established the computational expression of Nusselt number (N_{uB}) of the forced convection based on the condensation experimental data of R22 and R410A. Recently, Ali et al. [16–20] studied the effect of the wire thermal conductivity on the wire wrapped tubes for the condensation of steam. Solanki et al. [21] investigated the condensation heat transfer coefficients and frictional pressure drops of R-134a inside a micro-fin helical coiled tube experimentally. In their study, the cooling water flowed inside the shell in the opposite flow direction. Ammar et al. [22] obtained the condensation frictional pressure drop in the multiport micro channel smooth and grooved flat tubes using R134a. Park et al. [23] carried out a comprehensive study of the condensation heat transfer coefficients on the horizontal plain tube using a wide range of available different refrigerants. Moreover, Du et al. [24] conducted a numerical simulation and optimized a mid-temperature heat pipe exchanger. Based on parallel compressors with consideration of the volumetric and isentropic efficiency, Shen et al. [25] analyzed the performances of unit refrigeration systems. Furthermore, they proposed a novel model for the characterization of the frozen soil and correlated latent heat effects for the improvement of the ground freezing techniques [26]. Ancellin et al. [27] simulated violent separated flows with the liquid-vapor phase-change interface conditions.

Performed literature survey indicates that although many experimental and theoretical studies have been carried out so far about the heat transfer characteristics in heat exchanger tubes, the majority of theoretical models are based on the old refrigerants, while refrigerants that have been recently developed have not been analyzed by the relevant theoretical models yet. Considering these shortcomings, in the present study, it is intended to analyze the heat transfer mechanism in micro-finned tubes. To this end, experiments will be carried out to investigate the condensation heat transfer of R1234yf in a two-phase flow. Moreover, the condensation heat transfer characteristics of R1234yf in smooth and micro-finned tubes will be simulated by theoretical models. Finally, the prediction accuracy of the theoretical model will be evaluated, which would provide a theoretical support and experimental guidance for heat exchanger heat transfer enhancement analysis.

2 Experimental Device

Fig. 1 illustrates the design principle of the test-bed. The main components of the test-bed include the liquid reservoir, refrigerant pump, mass flowmeter, preheater, experimental section, condenser, electromagnetic flowmeter, water pump, refrigeration unit, and so on. By adjusting the electric heating voltage and current in the preheater, the refrigerant two-phase state at the entrance of the experimental section can be realized. Moreover, the refrigerant of the two-phase condensation experiment can be flowed into the condenser after throttling by the electronic expansion valve for the supercooling treatment. It should be indicated that the refrigerant state at the outlet of the experimental section can be determined by the refrigerant state at the outlet of the condenser and the heat transfer capacity of the condenser.

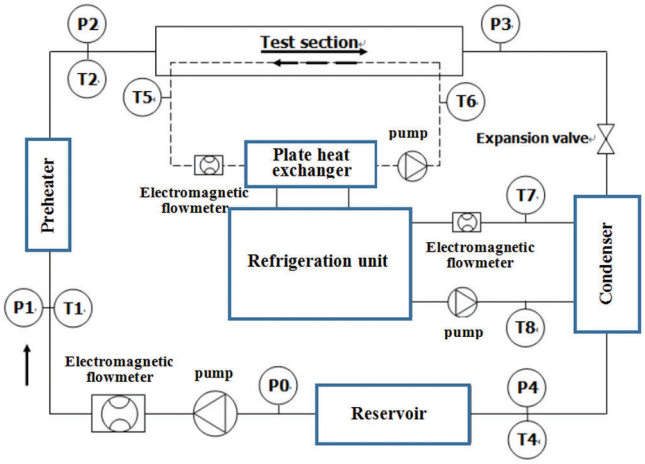

Figure 1: Schematic diagram of the test-bed

In the experimental system, WZPM-201 PT100 platinum resistance is selected to measure the refrigerant and water temperature in the system. It should be indicated that the measuring range and the measuring accuracies are 0–150°C and 0.1°C, respectively. Moreover, the 76 um T thermocouple is selected to measure the wall temperature of the heat exchanger tube, which is arranged in the same cross-section of the heat exchanger tube in four directions. Furthermore, the Hke-3051GP pressure transmitter is utilized to measure the refrigerant pressure in the system. It is worth noting that the measuring range and the measuring accuracies are 0–42 bar and 0.5%, respectively. The Coriolis DMF-1 mass flowmeter is used to measure the refrigerant circulation flow. The measurement accuracy and the measurement range are 0.15% and 0–200 (kg/h), respectively. Red flag HQ-LWG electromagnetic flowmeter is selected to measure the water circulation flow. The measuring accuracy level and the measuring range are 0.5 and 0–500 (m^3/h), respectively.

The experimental section is a tube heat exchanger. Fig. 2 shows that the refrigerant is condensed inside the heat exchanger tube, and the chilled water flows in the annular channel. The heat exchanger tube mainly consists of one smooth tube and two inner threaded tubes. Fig. 3 illustrates the cross-section of the inner threaded tube.

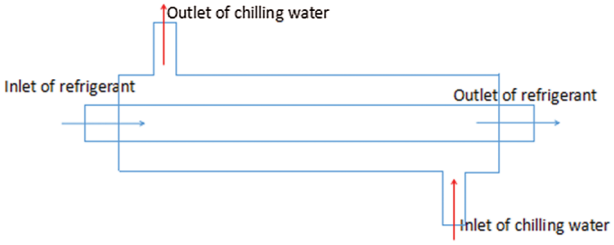

Figure 2: Configuration of the test section

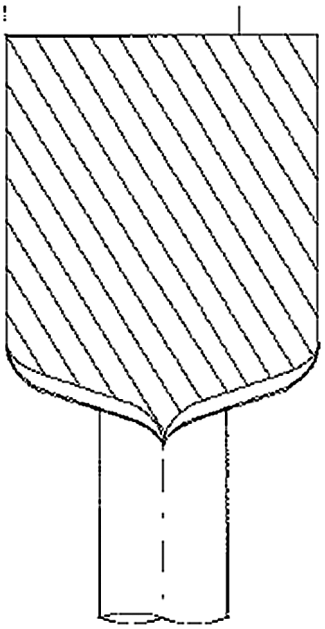

Figure 3: Cross-section of the internally ribbed tube

Tab. 1 presents the structural parameters of the heat exchanger tube.

Table 1: Structural parameters of the heat transfer tube

Tube type	Smooth tube	$1^{\#}$ internally ribbed tube	$2^{\#}$ internally ribbed tube
Internal diameter (mm)	3.5	3.5	3.5
Helical angle (°)	–	8	15
Rib height (mm)	–	0.2	0.25
Rib number	–	60	60
Tooth apex angle (°)	–	40	40
Pitch (mm)	–	0.183	0.183

3 Experimental Data Processing

The system contains many heat exchanger elements, including the preheater, condenser, refrigeration unit and plate heat exchanger. However, the electric heating in the preheater provides heat input for the system and cooling capacity for the refrigeration unit as the heat output of the system, while the other parts are heat transfer carriers.

At the inlet of the heat exchanger tube, the enthalpy of the refrigerant is mathematically expressed as:

$$H_{in} = H_1 + Q_{pre}/m_r \tag{1}$$

where:

H_1 is the refrigerant enthalpy at the inlet of the preheater, which can be calculated by measuring the temperature and pressure, kJ/kg.

H_{in} is the enthalpy of the refrigerant at the inlet of the test-section, kJ/kg.

Q_{Pre} is the amount of the refrigerant heating in the preheater, which is mainly controlled by adjusting the voltage and current, kW.

m_r is the mass flow rate of the refrigerant in the system, kg/s.

Moreover, at the outlet of the heat exchanger tube, the enthalpy of the refrigerant is:

$$H_{out} = H_4 + Q_{con}/m_r \tag{2}$$

where:

H_{out} is the refrigerant enthalpy at the outlet of the heat exchanger tube, kJ/kg.

H_4 is the refrigerant enthalpy at the outlet of the condenser. It can be calculated from the measured temperature and pressure, kJ/kg.

Q_{con} is the heat transfer in the condenser. It can be adjusted by the measured water flow and the inlet and outlet water temperature, kW.

Therefore, the dry degree of the refrigerant at the inlet of the heat exchanger tube is described as follows:

$$x_{in} = (H_{in} - H_l)/h_{fg} \tag{3}$$

The dryness of the refrigerant at the outlet of the heat exchanger tube is as follows:

$$x_{out} = (H_{out} - H_l)/h_{fg} \tag{4}$$

where:

H_l is the liquid enthalpy of the refrigerant at the saturated pressure, kJ/kg.

h_{fg} is the latent heat value of the refrigerant gasification under the saturated pressure, kJ/kg.

The arithmetic average of the refrigerant dryness at the inlet and outlet of the heat exchanger tube is used as the calculation standard of the heat exchanger dryness in the tube, which is expressed as follows:

$$x_{\mathrm{a}} = (x_{\mathrm{out}} + x_{\mathrm{in}})/2 \tag{5}$$

Thermocouples are mainly arranged on the outside surface of the heat exchanger tubes. The temperature difference between the inside and outside surface of the heat exchanger tubes is as follows:

$$\Delta T_w = m_r(H_{in} - H_{out}) \ln(D_o/D_i)/(2\pi\lambda l) \tag{6}$$

where:

λ is the thermal conductivity of the heat exchanger tube, W/(m K);

l is the effective heat transfer length, m.

In summary, the heat transfer coefficient [10] in the tube is as follows:

$$h_r = m_r(H_{in} - H_{out})/A_i(T_s - T_{win}) \tag{7}$$

where:

T_{win} is the inner wall temperature of the heat exchanger tube, °C, $T_{win} = T_{out} - \Delta T_w$.

T_{wout} is the outer wall temperature of the heat exchanger tube, °C.

T_s is the saturation temperature of the heat transfer in the tube, °C.

A_i is the surface area of the heat exchanger tube, m^2.

4 Analysis of Experimental Data

In the present study, R1234yf is selected as the refrigerant. Conditions are set as follows: The condensation temperature is 40°C, 43°C and 45°C, the refrigerant mass flow rate is 500 kg/(m^2·s)–900 kg/(m^2·s) and the refrigerant dryness at the inlet and outlet of the heat exchanger tube is set to 0.8–0.9, 0.2–0.3.

The influence of the mass flow rate, condensation temperature and spiral angle of fins on the heat transfer coefficient is experimentally analyzed. Then, the heat transfer coefficient in the tube is theoretically predicted by using the heat transfer correlation. The prediction accuracy is studied from two aspects, including the correlation fitting mechanism and the hypothetical condition of the heat transfer in the tube.

4.1 Experimental Analysis of the Heat Transfer Coefficient

Fig. 4 shows the variation of heat transfer coefficients with the mass flow rate and condensation temperature in 15° fin helical angle micro-ribbed tubes. It is observed that the mass flow rate is 500–900 kg/(m^2·s) and condensation temperatures are 40°C, 43°C and 45°C.

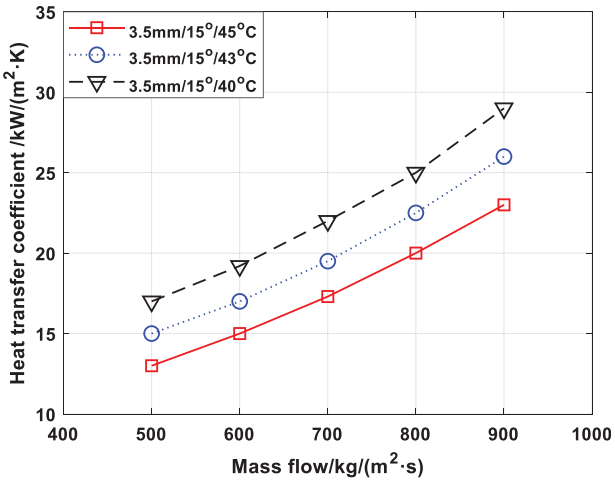

Figure 4: Influence of the condensation temperature on the heat transfer coefficient

Fig. 4 shows that the heat transfer coefficient increases as the condensation temperature decreases and the mass flow rate increases. The heat transfer coefficient increases by about 0.63–1.48 kW/(m^2·K) and about 3.85%–7.70% for each decrease of the condensation temperature by 1°C. Moreover, the heat transfer coefficient increases by about 2.23–3.47 kW/(m^2·K) and about 0.34%–0.45% for each increment of the mass flow rate by 100 kg/(m^2·s).

The gas-liquid flow rate increases as the mass flow rate increases, while the turbulence increases as the gas-liquid flow rate increases. In other words, the mass flow rate mainly enhances the heat transfer effect of the tube by enhancing the turbulence of the fluid. The condensation temperature mainly affects the heat transfer effect in the tube by affecting the physical properties of the refrigerant. The liquid film in the tube causes the main thermal resistance of the heat transfer between the vapor phase refrigerant and the chilled water.

The heat transfer coefficient of materials is measured by the unsteady plane heat source method. As the condensation temperature decreases, the heat transfer coefficient of the liquid refrigerant increases gradually. When the condensation temperature decreases by 1°C, the thermal conductivity increases by about 0.291–0.296 mW/(m·K).

Moreover, as the condensation temperature increases, the gas-liquid density ratio of the two-phase flow increases gradually by about 0.0167–0.0185. Moreover, the interfacial shear force decreases as the gas-liquid density ratio increases, which weakens the turbulence of the fluid in the tube. Therefore, it is found that the reduction of the condensation temperature is beneficial to the enhancement of the heat transfer effect.

Considering the flow and condensation heat transfer in the tube, fins can enhance the heat transfer effect mainly by three ways: (1) Increasing the effective heat transfer area in the tube, (2) Under the action of the surface tension, fins are beneficial to the rapid discharge of the condensate, (3) Fins enhance the turbulence of the two-phase flow in the tube through the disturbance of the two-phase flow [28].

Under different conditions, three heat transfer enhancement measurements play different roles. In the case of the low mass flow and high dryness, the effect of the fin accelerated condensate discharge on the heat transfer enhancement is more significant. On the other hand, in the case of high mass flow and low dryness, the disturbance of the fin to two-phase flow gradually becomes the main body of the heat transfer enhancement. Moreover, the increment of the heat transfer area always plays an important role in the process of heat transfer enhancement.

Fig. 5 illustrates the heat transfer enhancement effect of the micro-finned tubes under the experimental conditions of 500–900 kg/(m^2·s) mass flow rate and 43°C condensation temperature.

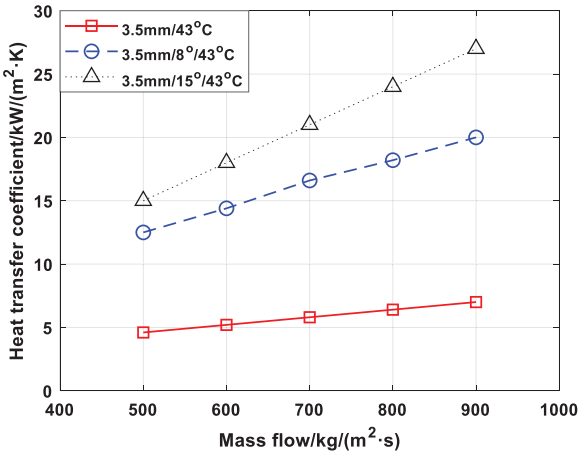

Figure 5: Influence of the fin helical angle on the heat transfer coefficient

It is observed that the heat transfer coefficient of 8° fin helical angle micro-fin tube is about 2.51–2.89 times that of the inner smooth tube. Moreover, the heat transfer enhancement ratio of 15° fin helical angle micro-fin tube is about 3.11–3.57 times. The heat transfer enhancement ratio increases as the mass flow rate increases. Moreover, the heat transfer enhancement ratio of both micro-fin tubes is higher than that of their area. The area increment rates of 8° and 15° fin helical angle micro-ribbed tubes are 2.29 and 3.08, respectively.

The heat transfer enhancement ratio is higher than the area increment ratio, which shows that fins not only enhance the heat transfer by increasing the effective heat transfer area, but also enhance the heat transfer mechanism of the fluid in the tube.

The two-phase flow in the micro-ribbed tube mainly includes two types: the circumferential rotational flow of the fluid below the fin height and the axial flow of the fluid above the fin height. The circumferential rotating velocity and the axial velocity increase as the mass flow rate increases, which results in the increment of the turbulence intensity in the two-phase flow.

4.2 Theoretical Analysis of the Heat Transfer Coefficient

The heat transfer correlations can be divided into two types, including the homogeneous correlations and fractional correlations. It should be indicated that the two-phase flow in the tube is regarded as a "single fluid", and the physical properties of the "single fluid" should be reasonably calculated by using the physical properties of the pure liquid phase and pure gas-phase fluids in combination with the specific experimental conditions. Therefore, the accuracy of the physical properties calculation of "single fluid" is of great importance for the accuracy of the correlation prediction.

The fractional correlation equation assumes that multiple correlations exist between the two-phase heat transfer coefficient and the single-phase heat transfer coefficient. It should be indicated that the coefficient is called the "conversion coefficient". Moreover, the determination of the conversion coefficient is important for the prediction accuracy of the fractional correlation equation [29].

In the experiment, correlations proposed by Cavallini et al. [30], Thome et al. [10], Dobson et al. [31] and Jung et al. [11] are used to predict the heat transfer coefficients in smooth tubes.

Cavallini et al. [30] utilize the whole liquid phase heat transfer coefficient h_{lo} at the same mass flow rate as the calculation standard. Moreover, the dimensionless gas velocity J_g is used to classify the flow pattern into the temperature-controlled flow pattern and non-temperature-controlled flow pattern. Combining with the experimental range of this study, the heat transfer coefficient calculation equation under the non-temperature controlled flow pattern is used to calculate the heat transfer characteristics in the optical tube, which is described as follows:

$$h_{tp} = h_{lo}\left(1 + 1.128x^{0.817}\left(\rho_1/\rho_g\right)^{0.3685}\left(u_1/u_g\right)^{0.2363}\left(1 - u_1/u_g\right)^{2.144}\mathrm{Pr}_1^{-0.1}\right) \tag{8}$$

Thome et al. [10] defined the heat transfer forms of the drying zone and the wetting zone as the membrane condensation heat transfer (h_f) and the forced convection heat transfer (h_c), respectively. Finally, the proportion of the drying zone and wetting zone is calculated according to the experimental conditions. Then, the heat transfer coefficient in the tube is calculated as the following:

$$h_{tp} = \left(h_f r\theta + (2\pi - \theta)rh_c\right) \times 2\pi r \tag{9}$$

Dobson et al. [31] and Jung et al. [11] correlations are based on the liquid phase heat transfer coefficients in the two-phase flow. Moreover, it is assumed that the conversion coefficients are only functions of the parameter X_{tt}. Finally, the correlation between the conversion coefficient and the parameter X_{tt} is determined according to the experimental data as the following:

Dobson et al. [31] correlations:

$$h_{tp}/h_1 = 1 + 2.22/\mathrm{X}_{tt}^{0.89} \tag{10}$$

Jung et al. [11] correlations:

$$h_{tp}/h_1 = 22.4 \times (1 + 2/X_{tt})^{0.81} h_f m_r^{0.33} \tag{11}$$

Fig. 6 shows the predictive effect of four correlations on the heat transfer coefficient in the smooth tube.

It is observed that Cavallini et al. [30] correlation obtain the highest prediction accuracy for the heat transfer coefficient in the tube. The prediction error range and the average prediction error are within ±8% and 0.56%, respectively. The heat transfer coefficient in the tube is overestimated by Thome et al. Dobson et al. and Jung-correlations [10,11,31]. The prediction errors ranges are: −1.58%–25.44%, 2.34%–20.71%, 14.99%–35.78%, and the average prediction errors are 11.63%, 11.84% and 25.08, respectively.

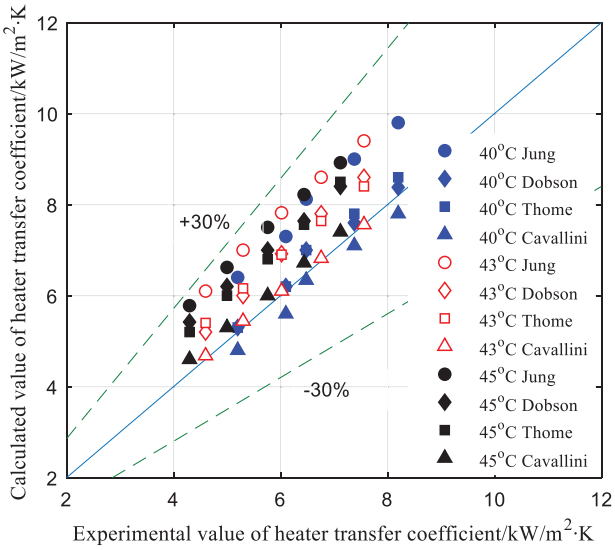

Figure 6: Prediction of the heat transfer coefficient inside the smooth tube by correlation

The main reason for overestimating the heat transfer characteristics in tubes is that the abovementioned correlations are mainly based on the fitting of the experimental data under the annular flow pattern [32–34]. In the present study, the fluid flow patterns in the heat exchanger tubes include plug flow, slug flow, annular flow, mist flow and so on. In other words, the heat transfer characteristics in part of the heat transfer area in heat exchanger tubes are worse than the annular flow. The calculated value of the correlation is higher than the experimental value of the heat transfer coefficient.

Moreover, the prediction accuracy of Dobson et al. correlation [31] and Jung et al. [11] correlation is significantly affected by the condensation temperature, while that of Thome et al. correlation is less affected by experimental variables.

In the experiment, Cavallini et al. Oliver et al. Miyara et al. Koyama et al. Goto et al. [35] and Tang et al. [36] correlations are used to predict the heat transfer coefficient in the inner screw tube [12–15,35,36].

Where Re_{eq} and R_x are used to characterize the turbulence effect of the two-phase flow in micro-finned tubes and the enhancement effect of fins on the heat transfer in micro-finned tubes. Moreover, bond number B_o and Froude number F_r are used to characterize the effects of shear force, gravity and surface tension of two-phase flow on heat transfer in tubes in Cavallini et al. [12] and Oliver et al. [13] correlations, respectively. Finally, based on the experimental data, the correlation between the dimensionless variables in the correlation is determined. Cavallini et al. correlation [12] can predict the heat transfer coefficients of multi-dentate tubes, such as internally threaded tubes and herringbone tubes. Meanwhile, Oliver et al. correlation [13] is mainly applicable to the prediction of the heat transfer coefficients of stratified and annular flow patterns in micro-finned tubes [13,30].

Furthermore, it is found that both Cavallini et al. [12] and Oliver et al. [13] correlations overestimate the heat transfer coefficients in tubes, and the prediction errors of the correlation for heat transfer coefficients in 8° fin helical angle micro-fin tubes are less than 15° fin helical angle micro-fin tubes [13,30].

The prediction deviations of the correlation equation are significantly affected by the mass flow rate, condensation temperature and fin structure. Fig. 7 shows that prediction errors range from –9.03% to 18.74%, from 15.56% to 79.56%, and the average prediction deviations are 6.54% and 43.69%, respectively.

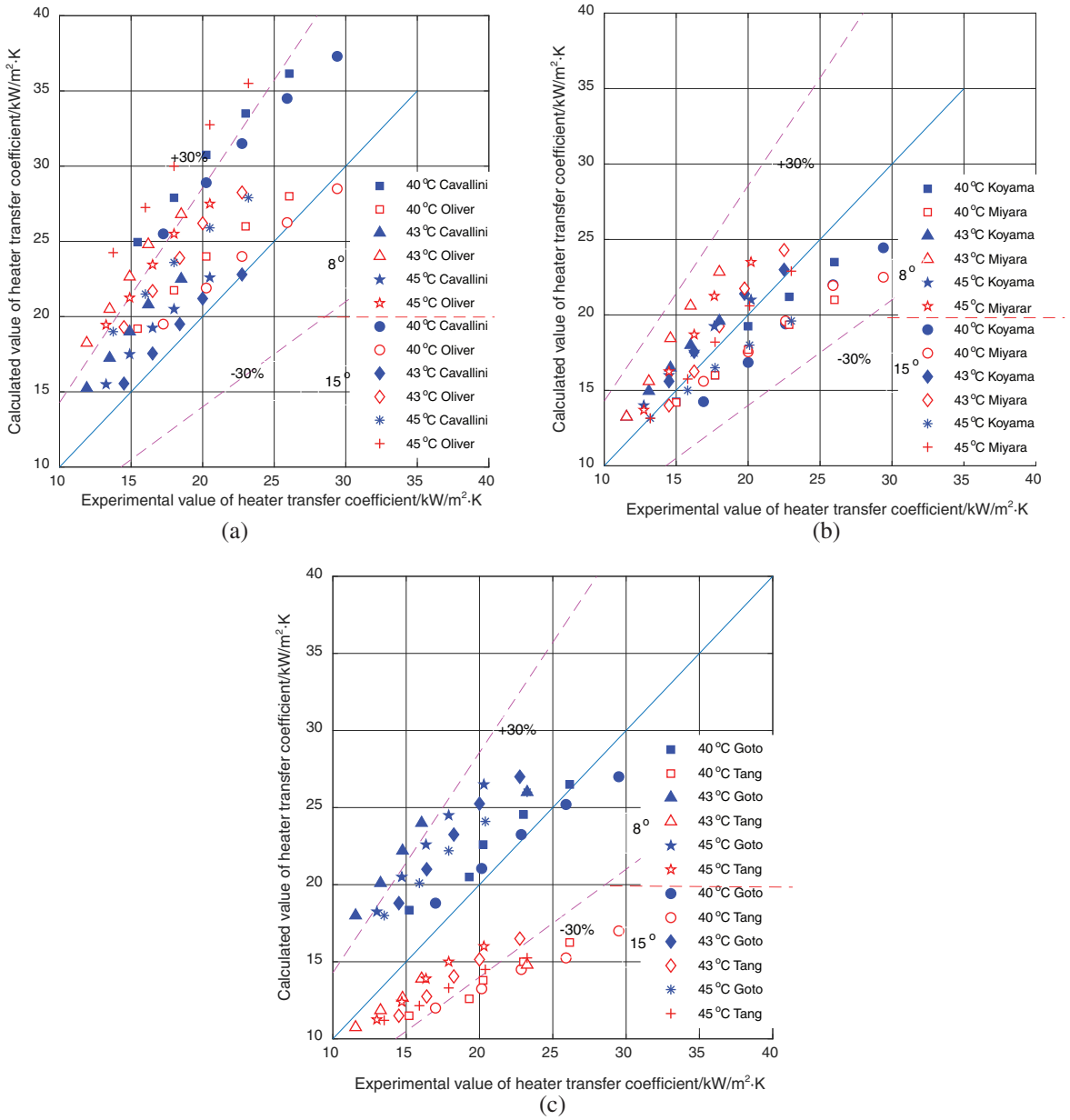

Figure 7: Prediction of the heat transfer coefficient inside the internally ribbed tube by correlation (a) Cavallini et al. [12] & Oliver et al. [13] correlation (b) Miyara et al. [14] & Koyama et al. [15] correlation (c) Goto et al. [35] & Tang et al. [36] correlation

It should be indicated that the Miyara et al. correlation [14] is an improved Koyama et al. correlation, [15] which is mainly applicable to the prediction of heat transfer coefficients in herringbone tubes. On the other hand, the Koyama et al. correlation [15] is mainly applicable to heat transfer coefficients in internally threaded tubes. In the correlation, Koyama et al. [15] and Miyara et al. [14] categorize the heat transfer in the tube into the forced convection heat transfer (N_{uB}) of the fluid itself and forced convection heat transfer (N_{uF}) caused by fins [14,15]. It is worth noting that the enhancement of the heat transfer effect by fins in the micro-fin tube can be calculated by the forced convection Nussel number N_{uF}. The

accuracy of the Nu_F equation is to determine the expression of the conversion coefficient Φ_V. t The conversion coefficient Φ_V of Koyama et al. [15] correlation is mathematically expressed as:

$$\Phi_V = 1.1 + 1.3\left(GX_{tt}/(gd_i\rho_v(\rho_i - \rho_v))^{0.5}\right)^{0.35} \tag{12}$$

Moreover, the conversion coefficient Φ_V of Miyara et al. correlation [14] is described as the following:

$$\Phi_V = 1.2 + 1.65\left(GX_{tt}/(gd_i\rho_v(\rho_l - \rho_v))^{0.5}\right)^{0.35} \tag{13}$$

Fig. 7b shows the predictive effect of Miyara et al. and Koyama et al. correlations on heat transfer coefficients in Micro-finned tubes [14,15]. The obtained results show that the correlation has a reasonable prediction effect on the heat transfer coefficient in the tube. The prediction errors of the abovementioned correlations range from –26.98% to 7.79% and –20.21% to 26.06%, respectively. Moreover, the average prediction errors are –5.72% and 0.77%, respectively.

The predicted results of the Miyara et al. correlation [14] are not consistent with the experimental results. Moreover, the heat transfer coefficient in the herringbone tube is higher than that in the inner-thread tube. This is because the heat transfer efficiency of the herringbone fin and the inner-thread fin is similar to that of the inner-thread fin under the condition of the large mass flow, and the difference of the heat transfer efficiency between different teeth is small.

The predictive effect of the Koyamaet et al. correlation based on the fitting of the experimental data in the internally threaded tube is consistent with the experimental results. This proves the practicability of the Koyama et al. correlation [15] .

Goto et al. [35] also assumed that the fins in the tube are mainly characterized by the forced convection heat transfer (Nu_F). Moreover, it is assumed that the conversion coefficient Φ_V is only a function of the parameter X_{tt}. Finally, Nu_F expression of the convection heat transfer is obtained by the heat transfer coefficient in the herringbone tube.

Tang et al. [36] utilized the hydraulic diameter D_h to characterize the effect of the fin structure parameters on the turbulence of two-phase flow in the tube. Moreover, the pressure ratio (P_r/P_c) is used to characterize the heat transfer mechanism of the two-phase flow in the main tube. Based on the correlation of the heat transfer coefficient in the smooth tube, the results are as follows:

$$Nu = 0.023\mathrm{Re}_{ld}\mathrm{Pr}_l^{0.4}(C + a(x/(1-x))(-\ln\mathrm{Pr}_d)^n) \tag{14}$$

When the heat exchange tube is an internal threaded tube, we have the following parameters: $a = 210.19$, $C = 24$, $d = 0.48$, $n = 0.72$.

Fig. 7c shows the predictive effect of G-correlation and T-correlation on the heat transfer coefficient in internally threaded tubes. It is observed that:

The predicted value of Goto et al. correlation [35] is higher than the experimental value of the heat transfer coefficient. In other words, Goto et al. correlation [35] can obtain a reasonable prediction of the heat transfer coefficient in internally threaded tubes. It should be indicated that the predicted error ranges from –7.59% to 40.15%, and the average predicted error is 21.49%.

Tang et al. correlation [36] underestimates the heat transfer coefficient in the tube. Moreover, as the mass flow rate and spiral angle of fins increase, error between the predicted value and experimental value increases gradually. Therefore, it is found that the hydraulic diameter D_h cannot fully characterize the effect of the fin structure on the turbulence in the tube. The prediction error range of Tang et al. correlation [36] is –41.96%–7.02%, and the average prediction error is –24.24%.

5 Conclusions

In the present study, the two-phase flow condensation heat transfer experiment of R1234yf is carried out inside one smooth tube and two micro-fin tubes. The experimental results show that:

(1) The heat transfer coefficient increases as the condensation temperature decreases and the mass flow rate increases. Moreover, the heat transfer coefficient in the micro-finned tube is larger than that in the optical tube. The heat transfer enhancement ratios of 8° and 15° finned helical angle micro-finned tubes are 2.51–2.89 and 3.11–3.57, respectively. The heat transfer enhancement ratios are higher than the area increment ratios.

(2) For the heat transfer coefficient in smooth tubes, the Cavallini et al. correlation [12] has the highest prediction accuracy, and its prediction error range and the average prediction error are within ±8% and 0.56%, respectively. Thome et al. correlation [10], Dobson et al. correlation [31] and Jung correlation [11] all overestimate the heat transfer coefficient in tubes. Moreover, the average prediction error of the three correlation formulas is more than 10%.

(3) Both Cavallini et al. correlation [12] and Oliver et al. correlation [13] overestimate the heat transfer coefficient in micro-finned tubes. However, the prediction accuracy of Cavallini et al. correlation [12] is high, with an average error of 6.54%. Although prediction errors of Miyara et al. correlation [14] and Koyama et al. correlation [15] are small, the better prediction effect of Koyama et al correlation [15] is more convincing to the reliability of the experimental data. Moreover, Goto et al. correlation [35] overestimates the heat transfer characteristics in tubes, while Tang et al. correlation [36] underestimates the heat transfer characteristics in tubes. Therefore, none of them are suitable for predicting the heat transfer coefficients in internally threaded tubes.

Funding Statement: This work was supported by the National Natural Science Foundation of China (No. 41877251).

Conflicts of Interest: The authors declare that they have no conflicts of interest to report regarding the present study.

Nomenclature

a = 210.19, C = 24, d = 0.48, n = 0.72 parameter of Tang et al. [36] correlation of heat transfer coefficient

A_i: the surface area of heat exchanger tube, m^2

D_h: hydraulic diameter, m

H_1: the refrigerant enthalpy at the inlet of the preheater, kJ/kg

H_4: is the refrigerant enthalpy at the outlet of the condenser, kJ/kg

H_{in}: the enthalpy of refrigerant at the inlet of test-section, kJ/kg

H_{out}: the refrigerant enthalpy at the outlet of heat exchanger tube, kJ/kg

H_l: the liquid enthalpy of refrigerant at saturated pressure, kJ/kg

h_{fg}: the latent heat value of refrigerant gasification under saturated pressure, kJ/kg

h_f: the heat transfer form of drying zone as membrane condensation heat transfer, kJ/kg

h_c: the heat transfer form of wetting zone as forced convection heat transfer, kJ/kg

l: the effective heat transfer length, m

m_r: the mass flow rate of refrigerant in the system, kg/s

Nu_B: forced convection heat transferof fluid itself

Nu_F: forced convection heat transfer caused by fins

P_r/P_c: pressure ratio

Q_{con}: the heat transfer in the condenser, kW

Q_{pre}: the amount of refrigerant heating in the preheater, kW

T_s: the saturation temperature of heat transfer in tube, °C

T_{win}: the inner wall temperature of heat exchanger tube, °C, $T_{win} = T_{out} - \Delta T_w$

T_{wout}: the outer wall temperature of heat exchanger tube, °C
X_{tt}: Dobson et al. [31] and Jung [11] correlationsfunctions of the parameter
x_{in}: the dry degree of refrigerant at the inlet of heat exchanger tube
x_{out}: the dryness of refrigerant at the outlet of heat exchanger tube
λ: the thermal conductivity of heat exchanger tube, W/(m K)
Φ_V: conversion coefficient

References

1. Olivier, J. A., Liebenberg, L., Thorne, J. R., Meyer, J. P. (2007). Heat transfer, pressure drop, and flow pattern recognition during condensation inside smooth, helical micro-fin and herringbone tubes. *International of Refrigeration, 30(4),* 609–623. DOI 10.1016/j.ijrefrig.2006.11.003.
2. Pham, Q. V., Choi, K. I., Oh, J. T., Cho, H. (2018). Flow condensing heat transfer of R410A, R22, and R32 inside a micro-fin tube. *Experimental Heat Transfer, 32(2),* 102–115. DOI 10.1080/08916152.2018.1485783.
3. Singh, S., Kukreja, R. (2019). An experimental investigation of flow patterns during condensation of HFC refrigerants in horizontal micro-fin tubes. *International Journal of Air-Conditioning and Refrigeration, 27(1),* 1950010. DOI 10.1142/S201013251950010X.
4. Wang, M., Fan, G., Sun, Z. (2011). Heat transfer enhancement and optimal design of micro rib tube. *Petrochemical Equipment, 40(4),* 4–7.
5. Wu, X., Wang, X., Wang, W. (2003). Flow condensation heat transfer and pressure drop in horizontal micro-fin tubes. *Journal of Shanghai University of Science and Technology, 25(4),* 326–329.
6. Zheng, G., Song, J., Wu, X. (2007). Research on the impact of micro-fin tube geometrical parameters on condensation. *Refrigeration and Air Conditioning, 7(2),* 80–82.
7. Tang, S., Liu, X., Tao, W. (2007). Expermiental investigation on condensation heat transfer in horizontal microfin and smooth tube with refrigerant R22. *Journal of Zhengzhou Institute of Light Industry: Natural Science Edition, 22(1),* 42–45.
8. Krishnan, S., Suseel, J., Nagarajan, P. K. (2019). Convective thermal performance and entropy generation analysis on Solution Combustion synthesis derived magnesia nano-dispersion flow susceptible by a micro-fin tube. *Experimental Thermal and Fluid Science, 101,* 1–15. DOI 10.1016/j.expthermflusci.2018.10.002.
9. Kedzierski, M. A., Kang, D. (2018). Horizontal convective boiling of R1234yf, R134a, and R450A within a micro-fin tube. *International Journal of Refrigeration, 88,* 538–551. DOI 10.1016/j.ijrefrig.2018.02.021.
10. Thome, J. R., Hajal, J. E., Cavallini, A. (2003). Condensation in horizontal tubes, Part 2: New heat transfer model based on flow regimes. *International Journal of Heat & Mass Transfer, 46(18),* 3365–3387. DOI 10.1016/S0017-9310(03)00140-6.
11. Jung, D., Song, K. H., Cho, Y., Kim, S. J. (2003). Flow condensation heat transfer coefficients of pure refrigerants. *International Journal of Refrigeration, 26(1),* 4–11. DOI 10.1016/S0140-7007(02)00082-8.
12. Cavallini, A., Col, D. D., Doretti, L., Longo, G. A., Rossetto, L. (1999). A new computational procedure for heat transfer and pressure drop during refrigerant condensation inside enhanced tubes. *Journal of Enhanced Heat Transfer, 6(6),* 441–456. DOI 10.1615/JEnhHeatTransf.v6.i6.50.
13. Olivier, J. A., Liebenberg, L., Thome, J. R., Meyer, J. P. (2007). Heat transfer, pressure drop, and flow pattern recognition during condensation inside smooth, helical micro-fin, and herringbone tubes. *International Journal of Refrigeration, 30(4),* 609–623. DOI 10.1016/j.ijrefrig.2006.11.003.
14. Miyara, A., Nonaka, K., Taniguchi, M. (2000). Condensation heat transfer and flow pattern inside a herringbone-type micro-fin tube. *International Journal of Refrigeration, 23(2),* 141–152. DOI 10.1016/S0140-7007(99)00037-7.
15. Kim, Y., Seo, K., Jin, T. C. (2002). Evaporation heat transfer characteristics of R-410A in 7 and 9.52 mm smooth/micro-fin tubes. *International Journal of Refrigeration, 25(6),* 716–730. DOI 10.1016/S0140-7007(01)00070-6.
16. Ali, H. M., Qasim, M. Z. (2015). Free convection condensation of steam on horizontal wire wrapped tubes: Effect of wire thermal conductivity, pitch and diameter. *Applied Thermal Engineering, 90,* 207–214. DOI 10.1016/j.applthermaleng.2015.07.006.

17. Ali, H. M., Abubaker, M. (2015). Effect of circumferential pin thickness on condensate retention as a function of vapor velocity on horizontal pin-fin tubes. *Applied Thermal Engineering, 91,* 245–251. DOI 10.1016/j.applthermaleng.2015.08.025.
18. Ali, H. M., Qasim, M. Z., Ali, M. (2016). Free convection condensation heat transfer of steam on horizontal square wire wrapped tubes. *International Journal of Heat and Mass Transfer, 98,* 350–358. DOI 10.1016/j.ijheatmasstransfer.2016.03.053.
19. Ali, H., Kamran, M. S., Ali, H. M. (2017). Marangoni condensation of steam-ethanol mixtures on a horizontal low-finned tube. *Applied Thermal Engineering, 117,* 366–375. DOI 10.1016/j.applthermaleng.2017.02.016.
20. Ali, H., Kamran, M. S., Ali, H. (2018). Effect of condensate flow rate on retention angle on horizontal low-finned tubes. *Thermal Science, 22(1 Part B),* 435–441. DOI 10.2298/TSCI151128211A.
21. Solanki, A. K., Kumar, R. (2018). Condensation of R-134a inside micro-fin helical coiled tube-in-shell type heat exchanger. *Experimental Thermal and Fluid Science, 93,* 344–355. DOI 10.1016/j.expthermflusci.2018.01.021.
22. Ammar, S. M., Abbas, N., Abbas, S., Ali, H. M., Hussain, I. et al. (2019). Experimental investigation of condensation pressure drop of R134a in smooth and grooved multiport flat tubes of automotive heat exchanger. *International Journal of Heat and Mass Transfer, 130,* 1087–1095. DOI 10.1016/j.ijheatmasstransfer.2018.11.018.
23. Park, K. J., Kang, D. G., Jung, D. (2010). Condensation heat transfer coefficients of HFC245fa on a horizontal plain tube. *Journal of Mechanics Science Technological, 24(9),* 1911–1917. DOI 10.1007/s12206-010-0611-1.
24. Du, J., Wu, X., Li, R., Cheng, R. (2019). Numerical simulation and optimization of a mid-temperature heat pipe exchanger. *Fluid Dynamics & Materials Processing, 15(1),* 77–87. DOI 10.32604/fdmp.2019.05949.
25. Shen, D., Gui, C., Xia, J., Xue, S. (2020). Experimental analysis of the performances of unit refrigeration systems based on parallel compressors with consideration of the volumetric and isentropic efficiency. *Fluid Dynamics & Materials Processing, 16(3),* 489–500. DOI 10.32604/fdmp.2020.08969.
26. Shen, D., Si, H., Xia, J., Li, S. (2019). A new model for the characterization of frozen soil and related latent heat effects for the improvement of ground freezing techniques and its experimental verification. *Fluid Dynamics & Materials Processing, 15(1),* 63–76. DOI 10.32604/fdmp.2019.04799.
27. Ancellin, M., Brosset, L., Ghidaglia, J. (2020). On the liquid-vapor phase-change interface conditions for numerical simulation of violent separated flows. *Fluid Dynamics & Materials Processing, 16(2),* 359–381. DOI 10.32604/fdmp.2020.08642.
28. Wang, L. (2010). *Study on enhanced heat transfer technology of micro-rib tube heat exchanger*. Harbin Engineering University, Harbin, China.
29. Jia, S. (2018). *Study on the characteristics and models of HFO1234ze condensation heat transfer outside the reinforced tube on both sides*. Zhongyuan Institute of Technology, Zhengzhou, China.
30. Cavallini, A., Censi, G., Col, D. D., Doretti, L., Longo, G. A. et al. (2003). Condensation inside and outside smooth and enhanced tubes-a review of recent research. *International Journal of Refrigeration, 26(4),* 373–392. DOI 10.1016/S0140-7007(02)00150-0.
31. Dobson, M. K., Chato, J. C. (1998). Condensation in smooth horizontal tubes. *Journal of Heat Transfer, 120(1),* 193–213. DOI 10.1115/1.2830043.
32. Boisseux, X., Heikal, M. R., Johns, R. A. (2000). Two-phase heat transfer coefficients of three HFC refrigerants inside a horizontal smooth tube, part I: Evaporation. *International Journal of Refrigeration, 23(4),* 269–283. DOI 10.1016/S0140-7007(99)00056-0.
33. Saitoh, S., Dang, C., Nakamura, Y., Hihara, E. (2011). Boiling heat transfer of HFO-1234yf flowing in a smooth small-diameter tube. *Refrigeration, 34(8),* 1846–1853. DOI 10.1016/j.ijrefrig.2011.05.018.
34. Olsson, C. O., Sunden, B. (1998). Experimental study of flow and heat transfer in rib-roughened rectangular channels. *Experimental Thermal Fluid Science, 16(4),* 349–365. DOI 10.1016/S0894-1777(97)10034-6.
35. Goto, M., Inoue, N., Ishiwatari, N. (2003). Condensation and evaporation heat transfer of R410A inside internally grooved horizontal tubes. *International Journal of Refrigeration, 26(4),* 410–416. DOI 10.1016/S0140-7007(02)00153-6.
36. Tang, L., Ohadi, M. M., Johnson, A. T. (2000). Flow condensation in smooth and micro-fin tubes with HCFC-22, HFC-134a and HFC-410A refrigerants. Part I: Experimental results. *Journal of Enhanced Heat Transfer, 7(5),* 289–310. DOI 10.1615/JEnhHeatTransf.v7.i5.10.